Main Chain Ferrocenyl Amides from 1-Aminoferrocene-1′-carboxylic Acid

Katja Heinze*[a] and Manuela Schlenker[a]

Keywords: Metallocenes / Hydrogen bonds / Peptides / Conformation analysis

The non-natural amino acid 1-aminoferrocene-1′-carboxylic acid is synthesised from ferrocene in eight steps. The folding and association phenomena of amido-substituted ferrocenes in the crystal as well as in solution are studied by X-ray crystallography, IR and NMR spectroscopy and DFT calculations. The amino acid is selectively protected at the amino group with the use of the fluorenyl-9-methoxycarbonyl (Fmoc) group. An amide-linked ferrocene dimer is prepared using the HOBt/DCC protocol for amide formation. In the crystal the dimer forms a hydrogen-bonded sheet structure, while in solution dynamic intramolecular hydrogen bonds are observed by VT ^{1}H NMR and IR spectroscopy. The dynamic flipping process has been rationalised by DFT calculations.

Introduction

Natural materials are often superior to their artificial synthetic counterparts. The structural and functional variety of peptides is very impressive, especially when considering that only a few α-amino acids are incorporated. Introduction of non-natural amino acids into peptides may lead to novel biomaterials or hybrid materials with some properties that are similar to those of natural proteins such as folding, or with additional properties such as conductive, optical or magnetic properties.[1] The latter properties may be obtained through incorporation of transition metals in the main chain,[2] while folding and supramolecular organisation into stable conformations may be achieved by forming intra- and intermolecular hydrogen bonds to control morphological aspects e.g. formation of nanotubes,[3] fibres,[4] or hydrogels.[5]

Ferrocene derivatives[6] have advantageous characteristics such as excellent stability in water and air, and favourable electrochemical properties which have led to applications of ferrocene in molecular receptors, in sensor devices with electrochemical detection,[7−10] and in labelling of biomolecules.[11,12] Furthermore, the inter-ring separation of ferrocene of about 3.3 Å (close to the N···O distance in β-sheets of peptides) and the rotational freedom of the cyclopentadienyl rings has allowed to use ferrocene 1,1′-dicarboxylic acid as an organometallic β-turn mimetic in ferrocene conjugates of amino acids and peptides,[13−16] and as a molecular pair of scissors.[17]

In our approach peptides with ferrocene moieties in the backbone are sequentially built up by a stepwise synthesis giving a well-defined chain length and a primary structure of the peptide which allows full structural characterisation by NMR spectroscopic methods and X-ray crystallography, as well as high-level calculations. The key ferrocene building block is the non-natural amino acid 1-aminoferrocene-1′-carboxylic acid. Its optimised synthesis and the full characterisation of all intermediates using X-ray structural techniques, VT NMR spectroscopy[18] and DFT calculations is reported here, along with the application of fluorenyl-9-methoxycarbonyl (Fmoc)[19] solution-phase chemistry for *N*-protection and acid activation via benzotriazole ester.

Results and Discussion

Synthesis of 1-Aminoferrocene-1′-carboxylic Acid, Hydrochloride

In 1998 the first synthesis of 1-aminoferrocene-1′-carboxylic acid **9** was reported by Butler and Quayle.[20] However, the method yielded a mixture of compounds which could not be separated and purified. In the same year a different synthetic approach was used by Ueyama et. al, which gave pure 1-aminoferrocene-1′-carboxylic acid, hydrochloride **9** but in quite a low yield (28% from **6**[21]). As the yields of the reactions were unsatisfactory for a broader investigation and only few spectroscopic data were given,[20−22] we report on the optimised synthesis (51% from **6**) and detailed characterisation of **9** and all synthetic intermediates.

Scheme 1 summarises the reaction sequence starting from ferrocene **1** to give 1-aminoferrocene-1′-carboxylic acid, hydrochloride **9·HCl**. The key synthon in this synthesis is 1-aminoferrocene (**5**). Although aminoferrocene is a known compound, the main drawback for further preparative work is the tedious multistage preparation starting from ferro-

[a] Anorganisch-Chemisches Institut der Universität Heidelberg, Im Neuenheimer Feld 270, 69120 Heidelberg, Germany
Fax: (internat.) + 49-6221-545707
E-mail: katja.heinze@urz.uni-heidelberg.de

Supporting information for this article is available on the WWW under http://www.eurjic.org or from the author.

  DOI: 10.1002/ejic.200300897

cene, with ferrocenylazide[23,24], *N*-ferrocenylacetamide[25] or *N*-ferrocenylphthalimide[26] as key intermediates. The best method for a multigram synthesis of aminoferrocene proves to be the Gabriel synthesis from *N*-ferrocenylphthalimide (**4**), although this route necessitates the synthesis of 1-haloferrocene or ferrocene boronic acid as precursors of **4**. A high-yield synthesis of iodoferrocene **3** has been reported by Bildstein et. al.[26] starting with the selective mono-lithiation of ferrocene **1** with *t*BuLi, then isolating the solid lithio-ferrocene **2** and quenching of **2** with iodine. The reaction in pyridine of **3** with phthalimide and Cu_2O as catalyst has been reported to give the *N*-ferrocenylphthalimide **4**.[26] However, the reaction is accompanied by the formation of biferrocenes by copper-mediated C−C coupling even in the presence of excess phthalimide. The product **4** is thus contaminated with biferrocenes and phthalimide which could not be removed. To circumvent these problems, **4** is prepared in the absence of solvent directly from **3** and pre-formed Cu−phthalimide.[27,28] Hydrazinolysis of **4** in ethanol gives pure **5**, which is then *N*-acetylated with acetic anhydride to form 1-(acetylamino)ferrocene **6**. The *N*-acetylamino group deactivates the substituted Cp ring, allowing the selective Friedel−Crafts acylation of **6** with 2,6-dichlorobenzoyl chloride[21,24,29] at the unsubstituted Cp ring giving 1-(acetylamino)-1′-(2,6-dichlorobenzoyl)ferrocene (**7**). Basic hydrolysis of **7** introduces the desired COOH group seen in **8**. However, the yield of this reaction depends highly on the exact stoichiometric amount of added water. Removal of the acetyl protection group with hydrochloric acid furnishes the ferrocene-containing amino acid **9** as the hydrochloride.[21]

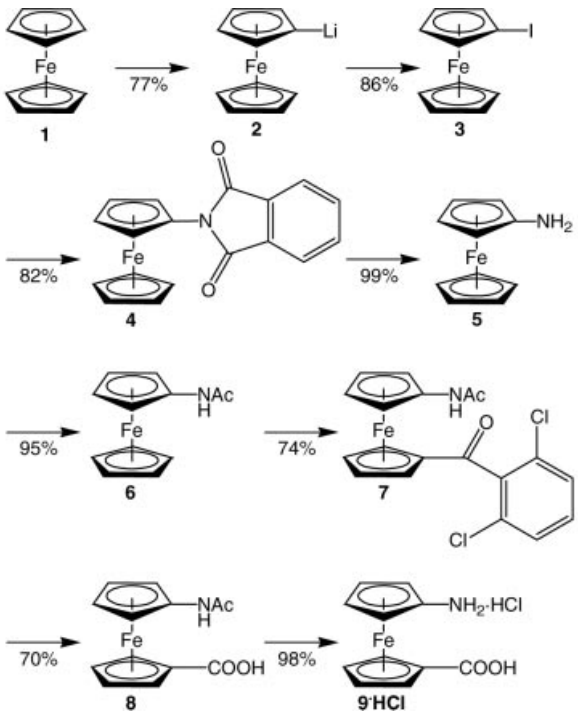

Scheme 1

Crystal Structures of 4-8

2-Ferrocenyl-isoindole-1,3-dione (**4**) crystallises in the monoclinic space group $P2_1/n$ without inclusion of solvent

Table 1. Selected bond lengths (Å) and angles (°) of complexes **4**, **5**, **6**, **7**, **8**, **10**, **11**, **12** and **13**

	4	**5**	**6**	**7**	**8**	**10**(A)	**10**(B)	**11**	**12**	**13**(Fe1)	**13**(Fe2)[d]
Fe1−C1	2.040(4)	2.097(3)	2.04(2)	2.101(3)	2.073(3)	2.064(2)	2.060(2)	2.067(4)	2.078(2)	2.082	2.087
Fe1−C2	2.044(4)	2.061(4)	2.05(2)	2.071(3)	2.056(4)	2.050(2)	2.061(2)	2.071(4)	2.069(3)	2.055	2.041
Fe1−C3	2.043(4)	2.033(4)	2.02(2)	2.044(4)	2.033(4)	2.037(2)	2.038(2)	2.043(4)	2.036(3)	2.019	2.026
Fe1−C4	2.033(4)	2.028(4)	2.02(2)	2.032(4)	2.041(4)	2.038(2)	2.036(2)	2.029(4)	2.033(2)	2.028	2.021
Fe1−C5	2.043(4)	2.056(4)	2.04(2)	2.051(3)	2.064(4)	2.043(2)	2.032(2)	2.037(4)	2.052(2)	2.039	2.032
Fe1−C6	2.039(4)	2.048(4)	2.07(2)	2.040(3)	2.043(4)	2.024(2)	2.023(2)	2.010(4)	2.047(2)	2.014	2.053
Fe1−C7	2.044(4)	2.051(4)	2.00(2)	2.050(4)	2.040(4)	2.033(2)	2.035(2)	2.017(4)	2.035(2)	2.032	2.053
Fe1−C8	2.042(4)	2.043(4)	2.03(2)	2.054(4)	2.047(4)	2.062(2)	2.063(2)	2.054(4)	2.045(3)	2.034	1.999
Fe1−C9	2.043(4)	2.042(4)	2.04(2)	2.053(4)	2.052(4)	2.059(2)	2.055(2)	2.061(4)	2.059(2)	2.017	2.002
Fe1−C10	2.032(4)	2.042(4)	2.04(2)	2.035(4)	2.035(4)	2.038(2)	2.041(2)	2.040(4)	2.058(2)	2.032	2.065
C1−N1	1.421(5)	1.405(5)	1.56(4)	1.405(4)	1.413(5)	1.407(2)	1.409(2)	1.399(5)	1.405(3)	1.395	1.408
N1−C11	1.416(5)	–	1.25(4)	1.351(5)	1.350(5)	1.349(2)	1.348(2)	1.370(6)	1.347(4)	1.347	1.370
N1−C12	1.409(5)	–	–	–	–	–	–	–	–	–	–
C11−O1	1.196(5)	–	1.26(4)	1.236(4)	1.228(5)	1.226(2)	1.225(2)	1.203(5)	1.233(3)	1.229	–
C12−O2	1.211(5)	–	–	–	–	–	–	–	–	–	–
C13−O2	–	–	–	1.221(4)	1.217(4)	1.252(2)	1.248(2)	1.206(4)	1.238(3)	–	–
C13−O3	–	–	–	–	1.335(5)	1.301(2)	1.300(2)	1.424(5)	–	–	–
N1−C11−O1	126.6(4)	–	126(4)	122.8(3)	122.5(4)	123.5(2)	123.3(2)	122.5(4)	123.0(2)	124.0	122.1
N1−C12−O2	125.6(4)	–	–	–	–	–	–	–	–	–	–
O2−C13−O3	–	–	–	–	122.9(4)	123.3(2)	123.6(2)	120.3(4)	–	–	–
C1−C5/subst1[a]	18.1	–	161.2	162.3	17.8	173.7	11.8	16.8	177.3	5.9	168.6
C6−C10/subst2[b]	–	–	–	13.4	174.2	172.5	7.0	171.6	36.3	178.3	–
δ[c]	−6.0	25.2	−34.6	−18.6	−4.8	16.3	11.2	21.0	8.2	−4.2	28.6

[a] Subst1 is the plane defined by the first three atoms of the substituent at C1. [b] Subst2 is the plane defined by the first three atoms of the substituent at C6. [c] δ is defined as the relative rotation of Cp rings (0° = fully eclipsed; 36° = fully staggered). [d] C1−C10, C11, N1, O1 stand for the atoms C21−C30, C13, N2, O2, respectively.

molecules (Figure 1). Bond lengths and angles in this compound compare well with similar systems (Table 1).[30] The plane of the phthalimido ring system is slightly rotated out of the adjacent Cp ring plane (angle between planes 18°). In a similar ferrocenyl-(2,3-naphthalimide) system with a CH_2 link between ferrocene and the naphthalimide, the substituent ring plane is located almost perpendicular to the Cp ring plane.[30]

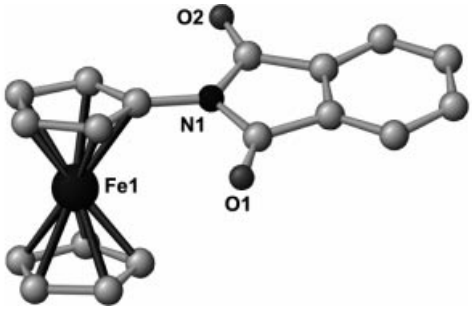

Figure 1. Molecular structure of **4** in the crystal

Aminoferrocene **5** crystallises in the tetragonal space group $I4_1/a$ (Figure 2). The bond lengths and angles are comparable with those found for 1,1′-diaminoferrocene (Table 1).[31] In the crystal the individual molecules of **5** are connected through N−H···N hydrogen bonds forming a helical arrangement along the crystallographic 4_1 screw axis (Figure 2) with a helical pitch of 5.93 Å (corresponding to the crystallographic *c*-axis). The N to N distance is 3.26 Å, and are in agreement with the distances found in the structure of 1,1′-diaminoferrocene (3.26, 3.10, 3.39 Å).[31]

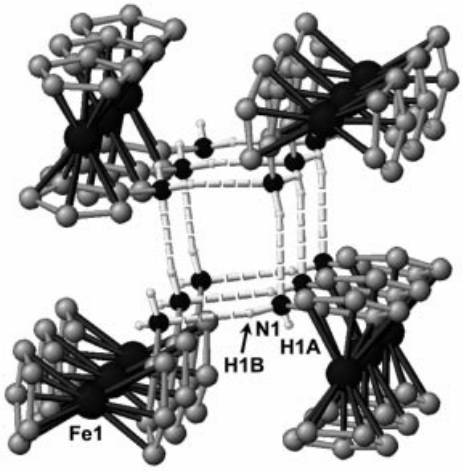

Figure 2. Hydrogen bonding of **5** in the crystal; view approximately along *c*

Compound **6** crystallises in the monoclinic space group $P2_1/n$ (Figure 3, Table 1). The molecules of **6** are connected through intermolecular N−H···O hydrogen bonds that connect the NH_{amide} group and the CO_{amide} group of a neighbouring molecule, forming chains along the *n* glide plane with a repeating distance of 9.54 Å (Figure 3). However, the $NH-CO-CH_3$ group is disordered over two positions, giving two different hydrogen bonds in the crystal: N1H1···O1X (N1 to O1X distance: 2.87 Å) and N1XH1X···O1 (N1X···O1 2.73 Å). A similar hydrogen-bonded chain has been observed in the related iodo-substituted complex $CpFeCpC(=O)NHCH_2I$ with a repeating distance of 9.55 Å and a N to O distance of 2.96 Å.[32]

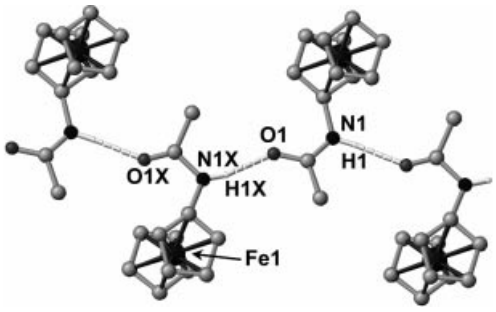

Figure 3. Hydrogen bonding of **6** in the crystal

The disubstituted ferrocene **7** crystallises in the monoclinic space group $P2_1/c$ (Figure 4, Table 1). Due to steric interactions the plane of the dichlorobenzene substituent is located almost perpendicular to the plane of the C6−C10 cyclopentadienyl ring (angle between planes: 82.9°). The molecules of **7** are connected through intermolecular N−H···O hydrogen bonds between the NH_{amide} group and the CO_{amide} group of a neighbouring molecule, forming chains along the 2_1 screw axis with a repeating distance of 9.02 Å; this is similar to that observed in structure **6** (Figure 3). The O1 to N1 distance is 2.88 Å and is similar to those found in **6** and the related complexes $H_3CC(=O)NHCpFeCpC(=O)NHCH_3$ (2.85 and 2.87 Å)[21] and $H_3CC(=O)NHCpFeCpC(=O)OCH_3$ (2.93 Å[33]).

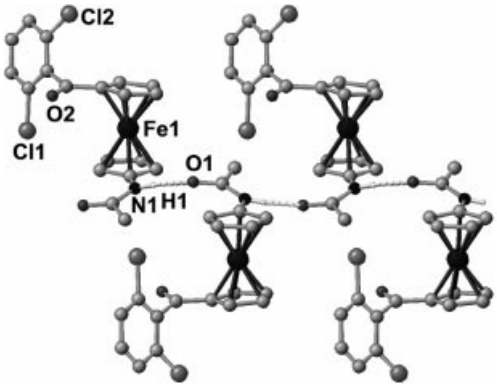

Figure 4. Hydrogen bonding of **7** in the crystal

The acid **8** crystallises in the orthorhombic space group *Pbca* with inclusion of one methanol molecule (Figure 5, Table 1). The ferrocene complexes are connected through O−H···O hydrogen bonds between the acid OH group (O3H6···O4; O3 to O4 distance: 2.56 Å) over the methanol and the amide CO group (O4H23···O1; O4 to O1 distance: 2.69 Å) to form a helical chain along a twofold axis (parallel to the *b* axis). These chains are further connected through NH···O hydrogen bonds between the amide NH group and the acid CO group (N1H1···O2; N1 to O2 distance: 2.91 Å). The same NH···O hydrogen-bonding motif has also been observed in the crystal structure of the corresponding methyl ester $H_3CC(=O)NHCpFeCp-C(=O)OCH_3$ that forms a dimer with an N to O distance of 2.93 Å.[33]

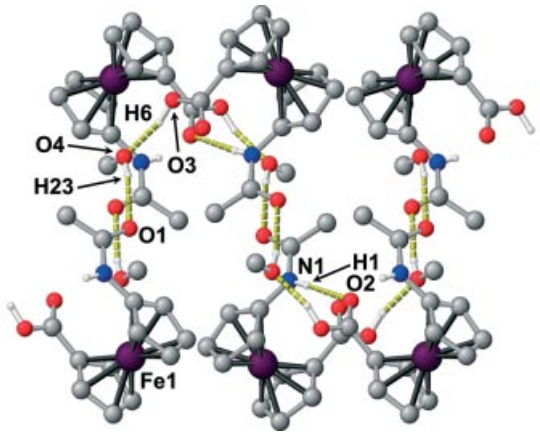

Figure 5. Hydrogen bonding of **8** in the crystal

Properties of 4−9

NMR spectroscopic data of compounds **4**−**13** are collected in Table 2 and Table 3, while UV/Vis spectroscopic and cyclic voltammetric data of **4**−**13** are given in Table 4.

In solution, the phthalimide substituent of **4** undergoes an easy torsional vibration around the C1−N1 bond leading to a time-averaged C_s symmetry of the molecule. Thus, in the ^1H and ^{13}C NMR spectra signal sets for a C_s-symmetric molecule are observed, e.g. only one ^{13}C resonance for the carbonyl carbon nuclei at δ = 167.0 is seen (Table 3; in contrast to the two erroneous reported values of δ = 165.1 and 167.0[26]). The IR absorption spectrum shows the signals assigned to the symmetric and asymmetric CO vibrations at 1778 cm^{-1} and 1717 cm^{-1}, respectively. In the UV/Vis spectrum of **4** bands corresponding to the ferrocene unit and to the phthalimide substituent are observed, and are in agreement with those reported for a similar ferrocenyl-1,8-naphthalimide (Table 4).[30] Further, the cyclic voltammogram of **4** displays waves corresponding to the oxidation of the ferrocene moiety at $E_{1/2}$ = 450 mV and the reduction of the phthalimide group at $E_{1/2}$ = −1470 mV (Table 4).[30]

The hydrogen bonding observed in the crystal of aminoferrocene **5** is also seen in the solid-state IR absorption spectrum: the signals for the NH stretching vibrations appear at 3400 cm^{-1} and 3336 cm^{-1}. The signal for the NH_2 deformation vibration is observed at 1621 cm^{-1}. In concen-

Table 2. ^1H NMR spectroscopic data of complexes **4**−**13**, atom numbering according to the numbering in the crystal structures

	$\Delta\delta_{NH\text{-}1}$[b]	H-1	H-2/5	H-3/4	H-7/10	H-8/9	H-12	Substituent(s)
4[b]	–	–	5.01		4.21 (br. s, 7 H)		–	7.74 (m, 2 H, H-15), 7.86 (m, 2 H, H-14)
5[b]	–	2.63 (br. s, 2 H)	3.98 (pt, 2 H)[a]	3.83 (pt, 2 H)[a]	4.09 (br. s, 5 H)		–	–
6[b]	−2.9	6.59 (br. s, 1 H)	4.53 (br. s, 2 H)	3.97 (br. s, 2 H)	4.15 (br. s, 5 H)		2.00 (s, 3 H)	–
7[b]	−3.4	6.73 (br. s,1 H)	4.69 br. s, 2 H)	4.15 (br. s, 2 H)	4.60 (br. s, 4 H)		2.02 (s, 3 H)	7.33−7.42 (m, 3 H, H-16/17/18)
8[b]	−12	7.15 (br. s, 1 H)	4.65 (br. s, 2 H)	4.07 (br. s, 2 H)	4.46/4.79 (br. s, 2 × 2 H)		2.11 (s, 3 H)	–
9[c]	–	–	4.30/4.51/4.63/4.89 (pt, 4 × 2 H)[a]				–	–
10[d]	−7.0	8.13 (br. s, 1 H)	4.55 (br. s, 2 H)	3.91 (br. s, 2 H)	4.25/4.66 (br. s, 2 × 2 H)		–	4.30 (br. s, 1 H, H-14), 4.47(d[e], 2 H, H-13), 7.32 (m, 4 H, H-17/18), 7.68 (d[f], 2 H, H-16), 7.78(d[f], 2 H, H-19)
11[b]	−3.9	7.42 (br. s, 1 H)	4.91 (br. s, 2 H)	4.15 (br. s, 2 H)	4.72/5.08 (br. s, 2 × 2 H)		1.90 (s, 3 H)	7.44−7.64 (m, 3 H, H-16/17/18), 8.08 (d[g], 1 H, H-15)
12[b]	−5.7	7.78 (br. s, 1 H)	4.44 (br. s, 2 H)	4.03 (br. s, 2 H)	4.34/4.66 (br. s, 2 × 2 H)		2.02 (s, 3 H)	1.05−1.80 (m, 20 H, Cy−CH_2), 3.48−3.59 (m, 1 H, H-15), 4.26 (m, 1 H, H-21), 5.88 (d[h], 1 H, NH)
13[b]	−6.6	7.13 (br. s, 1 H)	4.49 (br. s, 2 H)	4.17 (br. s, 2 H)	4.44/4.68 (br. s, 2 × 2 H)		2.10 (s, 3 H)	–
	−11	8.33 (br. s, 1 H)	4.89 (br. s, 2 H)	4.12 (br. s, 2 H)	4.26 (br. s, 5 H)		–	–

[a] A non-resolved duplet of duplets is denoted pseudo-triplet "pt". [b] In CD_2Cl_2. [c] In D_2O. [d] In $[D]_8THF$. [e] $^3J_{H,H}$ = 6.2 Hz. [f] $^3J_{H,H}$ = 6.8 Hz. [g] $^3J_{H,H}$ = 8.4 Hz. [h] $^3J_{H,H}$ = 7.4 Hz.

Table 3. ^{13}C NMR spectroscopic data of complexes **4**−**13**; atom numbering according to the numbering in the crystal structures

	C-1	C-2/5	C-3/4	C-6	C-7/10	C-8/9	C-11	C-12	C-13	Substituent(s)
4[a]	89.3	63.4	65.9		69.9		–	–	–	123.5 (C-14), 132.5 (C-13), 134.6 (C-15), 167.0 (C-11)
5[a]	106.5	58.7	63.6		69.2		–	–	–	–
6[b]	95.0	62.1	65.0		69.6		168.9	24.5	–	–
7[a]	96.3	64.1	67.5	80.6	71.8/74.6		168.9	24.1	197.3	129.0 (C-16), 131.1 (C-17), 132.3 (C-15), 138.9 (C-14)
8[c]	98.1	62.3	66.3	74.0	71.5/72.9		168.9	24.3	172.5	–
9[d]		63.7, 68.2, 70.5, 72.7, 81.3, 86.4					–	–	175.0	–
10[e]	99.1	61.2	65.9	73.2	71.3/72.3		–	–	171.6	47.9 (C-14), 120.1 (C-19), 125.4 (C-16), 127.3 and 127.8 (C-17/18), 141.8 (C-20), 144.8 (C-15), 154.0 (C-12)[f]
11[a]	98.6	63.4	67.2	65.6	72.4/74.9		169.4	24.0	167.3	109.2, 120.8, 125.5, 129.5 (C-15/16/17/18), 129.6, 144.1 (C-14/19)
12[a]	94.1	66.0	66.9	79.4	71.3/71.7		169.3	23.8	169.8	25.1, 25.9, 26.6, 31.4, 32.8 ($Cy-CH_2$), 50.7 (C-15), 55.7 (C-21)
13[e]	97.8	63.2	65.9	80.8	70.1/71.0		169.4	23.6	174.9	–
	98.3	61.5	64.4		69.6		–	–	–	–

[a] In CD_2Cl_2. [b] In $CDCl_3$. [c] In $[D]_8$DMSO. [d] In D_2O. [e] In $[D]_8$THF. [f] C^{13} under THF signal.

Table 4. UV/Vis and cyclic voltammetric data of complexes **4**−**13**

	λ_{max} (ε)[a]	λ_{max} (ε)[b]	$E_{1/2}$[c]	$E_{1/2}$[d]
4	443 (370)	325 (1670)	450	−1470
5	443 (195)	–	130	–
6	441 (215)	–	325	–
7	480 (755)	358 (1400)	585	−1480
8	441 (350)	–	525	–
9	431 (160)[e]	–	220[5)]	–
10	441 (230)	347 (590)	525	–
11	457 (430)	370 (555)	670	–
12	441 (450)[f]	–	465	–
13	451 (650)[f]	–	285/590	–

[a] λ_{max}(ferrocene) in nm, ε in $M^{-1}cm^{-1}$ in CH_2Cl_2; extinction conforms to Lambert-Beer's law in the concentration range 2−10 mM. [b] λ_{max}(substituent) in nm, ε in $M^{-1}cm^{-1}$ in CH_2Cl_2. [c] Oxidation $E_{1/2}$(ferrocene) in mV vs. SCE 10^{-3}M in $CH_3CN/n-Bu_4NPF_6$. [d] Reduction $E_{1/2}$(substituent) in mV vs. SCE 10^{-3}M in $CH_3CN/n-Bu_4NPF_6$. [e] In H_2O. [f] In THF.

Table 5. Characteristic IR spectroscopic data of the amide groups of complexes **6**, **7**, **8**, **11**, **12** and **13**

	6	**7**	**8**	**11**	**12**	**13**
amide A (solid)[a]	3262	3275	3322	3359	3319	3327/3316
amide A (CH_2Cl_2)[a]	3435	3431	3303	3428/3363	3291	3430/3292
amide I (solid)[b]	1655	1659	1666	1682	1672	1660/1646
amide I (CH_2Cl_2)[b]	1685	1687	1691	1689	1677	1679/1660
amide II (solid)[c]	1580	1574	1569	1548	1569	1560
amide II (CH_2Cl_2)[c]	1532	1531	1557	1536	1526	1559/1529

[a] Amide A = $\tilde{\nu}_{NH,stretching}$. [b] Amide I = $\tilde{\nu}_{CO,stretching} + \tilde{\nu}_{NH,bending} + \tilde{\nu}_{CN,stretching}$. [c] Amide II = $\tilde{\nu}_{NH,bending} + \tilde{\nu}_{CN,stretching}$.

trated solutions the bands of the NH stretching vibrations are slightly shifted to 3425 and 3354 cm^{-1} showing the presence of hydrogen bonding (in dilute solutions these bands are observed at 3757 and 3692 cm^{-1})[24]. Compound **5** is oxidised at +130 mV (vs. SCE), a much more positive potential than 1,1′-diaminoferrocene (approximately −200 mV vs. SCE[31]). Obviously, the electron-donating effect of the amino groups to the metal centre is additive.[34]

In the solid-state IR absorption spectrum of **6** the characteristic amide vibrations confirm the presence of hydrogen bonds (Table 5). In dilute solutions, however, the bands assigned to amide A and amide I are shifted to higher energies, while that of amide II is shifted to a lower energy, suggesting that hydrogen bonding is absent (Table 5). This finding is also corroborated by the ^1H NMR spectrum of **6** as the signal for the amide proton appears at δ = 6.59 in CD_2Cl_2 at 293 K (Table 2). A weak temperature dependence is indicative of either a non-bonded hydrogen atom or a hydrogen atom involved in a locked hydrogen bond.[13,18] For **6**, the weak temperature dependence of $\Delta\delta_{NH} = -2.9$ ppb K^{-1} is interpreted in terms of the absence of hydrogen bonding (Table 2); thus, **6** is not associated in solution. The cyclic voltammogram of **6** shows that it is oxidised at +325 mV (vs. SCE), a much more positive potential than the amino compound **5** (Table 4).

An IR spectroscopic investigation of **7** shows the presence of hydrogen bonds in the solid state, while in solution no hydrogen bonding is detected (Table 5). This is also verified by the ^1H chemical shift of the amide proton resonating at δ = 6.73 with $\Delta\delta_{NH} = -3.4$ ppb K^{-1} in CD_2Cl_2 (Table 2). Thus, **7** like **6** does not associate in solution. The UV/Vis absorption band for the ferrocene unit of **7** at 480 nm is probably admixed with a charge transfer component (from the electron-rich ferrocene to the electron-deficient aromatic system), and thus appears at a relatively low energy and with a high intensity (Table 4).[35] The absorption band for the aromatic substituent appears at 358 nm. The ferrocene moiety is oxidised at 585 mV and the aromatic substituent is reduced at −1480 mV (Table 4).

The hydrogen bonding observed in the crystal of **8** is also apparent in the solid-state IR absorption spectrum (Table 5). In solution the IR absorption data suggest a hydrogen bond involving the amide hydrogen atom (Table 5). In the proton NMR spectrum a signal at δ = 7.15 in CD_2Cl_2 (δ = 8.40 in THF, Table 2) is observed which is assigned to the amide proton on the basis of the NOESY spectrum (correlation between NH and CH_3). This low-field chemical shift as well as the large temperature depen-

dence $\Delta\delta_{NH} = -12$ ppb K^{-1} confirm that the NH proton is involved in a dynamic hydrogen bond in solution, which can arise from either intermolecular association or intramolecular folding processes.[13,18] The characteristic signal for the vibration of the acid carbonyl group appears at 1715 cm^{-1} in CH_2Cl_2 and in THF, and is similar to that found for ferrocenedicarboxylic acid (1720 cm^{-1} in THF), and suggests the formation of carboxylic acid dimers. As both functional groups are involved in hydrogen bonding, a dynamic intermolecular aggregation in solution is proposed (Scheme 2). The *cis* orientation of the amide groups necessary for intermolecular dimerisation (Scheme 2) is confirmed by NOESY spectroscopy (correlation peak between the CH_3 group and Cp protons H-2/5).

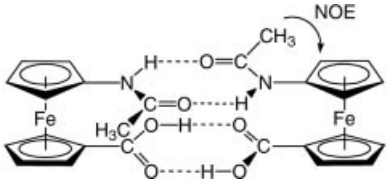

Scheme 2

DFT calculations (see Supporting Information) on monomeric **8** show that the non-hydrogen-bonded structure is the global minimum and the $O_{acid}-H\cdots O_{amide}$ hydrogen-bonded structure is a local minimum 13 kJ mol^{-1} higher in energy, while no minimum is found for the $N_{amide}-H\cdots O_{acid}$ hydrogen-bonded structure. However, the dimeric fourfold hydrogen-bonded structure is calculated to be a minimum 73 kJ mol^{-1} more stable than two isolated molecules of **8** (although this might be an overestimated stabilisation energy due to the basis set superposition error BSSE[36]), confirming the presence of intermolecular hydrogen bonds.

The amino acid **9** can be isolated as the hydrochloride salt **9·HCl** which is soluble and stable in water and dimethyl sulfoxide. Neutralisation of an aqueous solution of **9·HCl** with sodium hydroxide immediately leads to the precipitation of the zwitterionic compound, which rapidly decomposes to a black material at pH > 7. The solid-state IR absorption spectrum of **9·HCl** shows absorption bands that are assigned to the NH and OH groups at 3366, 3177 and 3135 cm^{-1}, indicating extensive hydrogen bonding which is probably intermolecular in nature. The UV/Vis absorption band for the ferrocene moiety of **9·HCl** appears at 431 nm, and is blue-shifted by more than 500 cm^{-1} relative to the bands of e.g. **4**−**6** (441−443 nm) probably due to the cationic nature of the complex.

Peptide Chemistry

A) N-Protection, Crystal and Solution Structure of 10

Since the stability of **9** in alkaline solution is rather poor, *N*-protection of **9** with fluorenyl-9-methyl chloroformate (Fmoc-Cl) has been carried out in buffered solution (phosphate buffer, pH 7) to give the *N*-protected amino acid 1-[(fluoren-9-yl)methyloxycarbonylamino]ferrocene-1′-carboxylic acid (**10**) (Scheme 3).

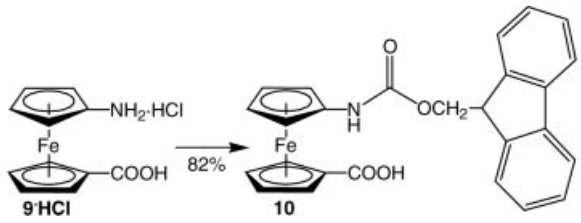

Scheme 3

Compound **10** crystallises in the monoclinic space group $P2_1/c$ with the inclusion of half a molecule dichloromethane per molecule (Figure 6, Table 1). The asymmetric unit contains two independent molecules **10(A)** and **10(B)** which are connected through double O−H···O hydrogen bonds involving the carboxylic acid functions (O3H6···O102, O3···O102 distance: 2.63 Å; O103H106···O2, O103···O2 distance: 2.59 Å) and double N−H···O hydrogen bonds involving the *cis*-orientated urethane HNCO groups (N1H1···O101; N1···O101 distance: 2.83 Å; N101H101···O1; N101-to-O1 distance: 2.86 Å) to form a dimer of approximate C_2 symmetry (Figure 6). The same two eight-membered rings have been detected in the crystal structure of the related Boc-protected complex HOOC−CpFeCpNH(C=O)O*t*Bu (Boc = *tert*-butoxycarbonyl) with O···O distances of 2.66 and 2.66 Å and N···O distances of 2.83 and 2.85 Å.[37] The planes of the fluorenyl substituents are located almost perpendicular to the planes of the cyclopentadienyl rings to which they are attached [**10(A)**: 91.2°, **10(B)**: 83.4°].

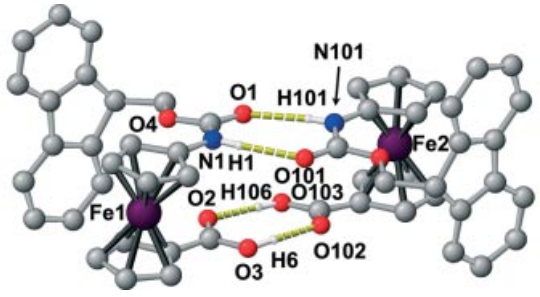

Figure 6. Hydrogen bonding of **10** in the crystal

The hydrogen bonding observed in the crystal of **10** is also confirmed by the IR absorption spectrum which shows the absorption bands assigned to the NH and OH groups between 3500−2800 cm^{-1}, signals for the carbonyl groups at 1707 (vs) and 1664 (s) cm^{-1}, and signals at 1560 (w) and 1544 (w) cm^{-1}. This pattern in the spectral region 1800−1500 cm^{-1} is in accordance with the pattern for a *cis*-orientation of the urethane moiety of **10** calculated by

DFT [1682 (1.00), 1668 (0.46), 1548 (0.11), 1510 (0.09) cm^{-1}; see Supporting Information].

In CH_2Cl_2 solution two dominant bands are observed at 1707 (vs) and 1673 (s) cm^{-1} and two weak bands at 1570 and 1542 cm^{-1}, suggesting that a *cis*-urethane conformation is the major species. In addition, a shoulder at 1735 cm^{-1} is observed indicating the presence of another species in CH_2Cl_2 solution. In THF solution, however, a different pattern is observed: 1735 (s), 1716 (s) and 1563 (s) cm^{-1}. DFT calculations on **10** with a *trans*-orientated urethane group predict a comparable pattern: 1715 (0.78), 1694 (0.67), 1569 (0.73) cm^{-1} (see Supporting Information). Thus, **10** prefers the *cis*-conformation in CH_2Cl_2 solution and in the crystal and the *trans*-conformation in THF.[38,39] In all cases the acid group appears to be hydrogen bonded via carboxylic acid dimers. In the NH/OH region of the IR absorption spectrum bands are observed at 3266, 3316 and 3425 cm^{-1} in CH_2Cl_2 and at 3269, 3504 and 3573 cm^{-1} in THF. Thus hydrogen bonding involving the NH group exists in CH_2Cl_2 and is absent in THF. NMR spectroscopy supports this interpretation: in CD_2Cl_2 solution two resonances[38,39] assigned to the NH protons are observed at δ = 6.95 (free NH group; *trans* conformation; $\Delta\delta_{NH}$ could not be determined as the signal moves into the multiplet for the fluorenyl protons) and δ = 7.99 (hydrogen-bonded NH group; *cis* conformation; $\Delta\delta_{NH} = -7$ ppb K^{-1}) with equal intensity, together with a doubled signal set for all Cp protons and the CH_2 group, while in THF solution only a single signal set for the NH, Cp and CH_2 protons is observed (Table 2). Based on the experimental data, the proposed dynamic solution structure of **10** is depicted in Scheme 4. The *cis*-orientated species which has the opportunity to form hydrogen bonds is the dominant species in CH_2Cl_2, while the *trans*-orientated conformer without NH hydrogen bonds is the major species in THF. These bonding motifs can be derived from the crystal structure of **10** (Figure 6) by cleaving one and two N−H···O hydrogen bonds, respectively, concomitant with a *cis*/*trans* rearrangement. A similar type of aggregation − albeit more stable − has been proposed for the similar complex **8** (Scheme 2).

B) COOH Activation, Crystal and Solution Structures of 11 and 12

Reaction of the *N*-acetylated amino acid **8** with 1-hydroxybenzotriazole (HOBt) in the presence of 1,3-dicyclohexylcarbodiimide (DCC) leads to the formation of the isolable ferrocenoyl benzotriazole ester **11** (Scheme 5). This reaction is similar to that of ferrocene carboxylic acid with HOBt/DCC.[40] In the absence of HOBt **8** reacts with

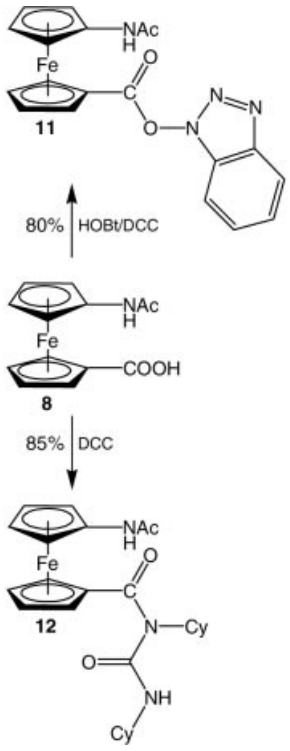

Scheme 5

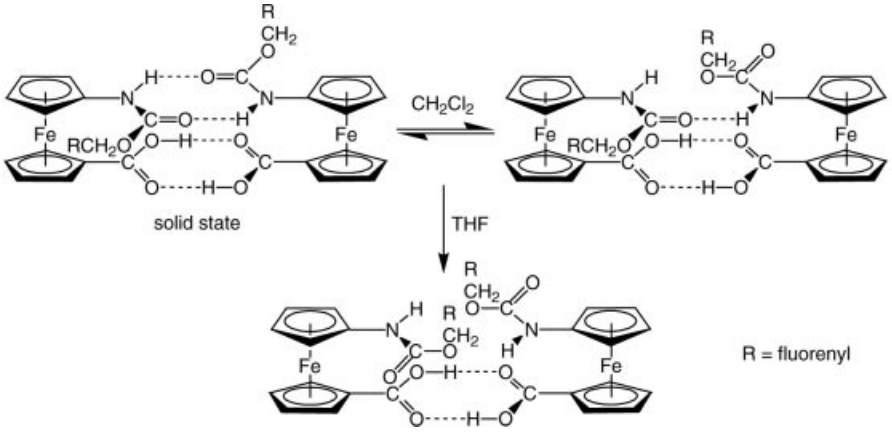

Scheme 4

DCC to give 1-[1′-(acetylamino)ferrocenylcarbonyl]-1,3-dicyclohexylurea (**12**) in a reaction similar to that of ferrocenecarboxylic acid with DCC.[41−43]

The activated ester **11** crystallises in the monoclinic space group $P2_1/n$ as discrete molecules (Table 1). The benzotriazole substituent is rotated out of the ester plane by 88.6°, similar to Fc-COOBt (96.6°[40]) but pointing in the opposite direction. This orientation allows for an intramolecular hydrogen bond from the amide NH to the central nitrogen atom of the Bt group (N1 to N3 distance: 3.06 Å, Figure 7).

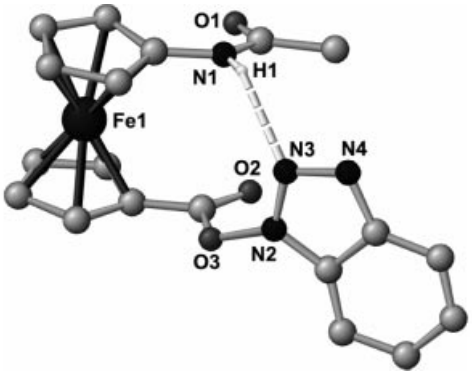

Figure 7. Molecular structure of **11** in the crystal

In the solid state the characteristic IR absorption bands of **11** appear at 3359 (amide A), 1764 (CO_{ester}), 1682 (amide I) and 1548 (amide II) cm^{-1}, while in solution these bands are shifted to 3428, 3363 (amide A), 1787 (CO_{ester}), 1689 (amide I) and 1536 (amide II) cm^{-1} (Table 5). These data show that in the solid state and in solution hydrogen bonding involving the NH part of the amide group occurs. DFT calculations suggest that the solution structure is identical to the crystal structure (Figure 8, see Supporting Information). This intramolecular hydrogen-bonded system is stabilised by 19 kJ mol^{-1} relative to the open form according to DFT calculations. The activation barrier for the hydrogen-bond dissociation is calculated to be 27 kJ mol^{-1}. This interpretation is supported by NMR spectroscopy: the signal for the amide proton appears at $\delta = 7.42$ in CD_2Cl_2 suggesting the presence of hydrogen bonding in dilute solution (Table 2). The signal is temperature dependent, with $\Delta\delta_{NH} = -3.4$ ppb K^{-1} when excluding intermolecular hydrogen bonding (a larger temperature dependence is expected when intermolecular hydrogen bonding is included[13,18]). In the VT-^{1}H NMR spectra the proton signals for the cyclopentadienyl rings H-2/5, H-3/4, H-7/10 and H-8/9 disappear at low temperature with a coalescence temperature (T_C) of 223, 213, 213 and 203 K, respectively, and reappear as separate signals with $\Delta\nu = 168$, 57, 39 and 9 Hz at lower temperature (Figure 8). This finding can be interpreted as a "frozen" interconversion of the enantiomeric hydrogen-bonded structures of **11** rendering the protons pairs H-2/5, H-3/4, H-7/10 and H-8/9 magnetically different (Figure 8). The activation barrier for this process can be estimated to be $\Delta G^{\neq}(T_C) = 43$ kJ mol^{-1}.

In the UV/Vis spectrum the absorption band for the ferrocene unit of **11** appears at 457 nm (probably admixed

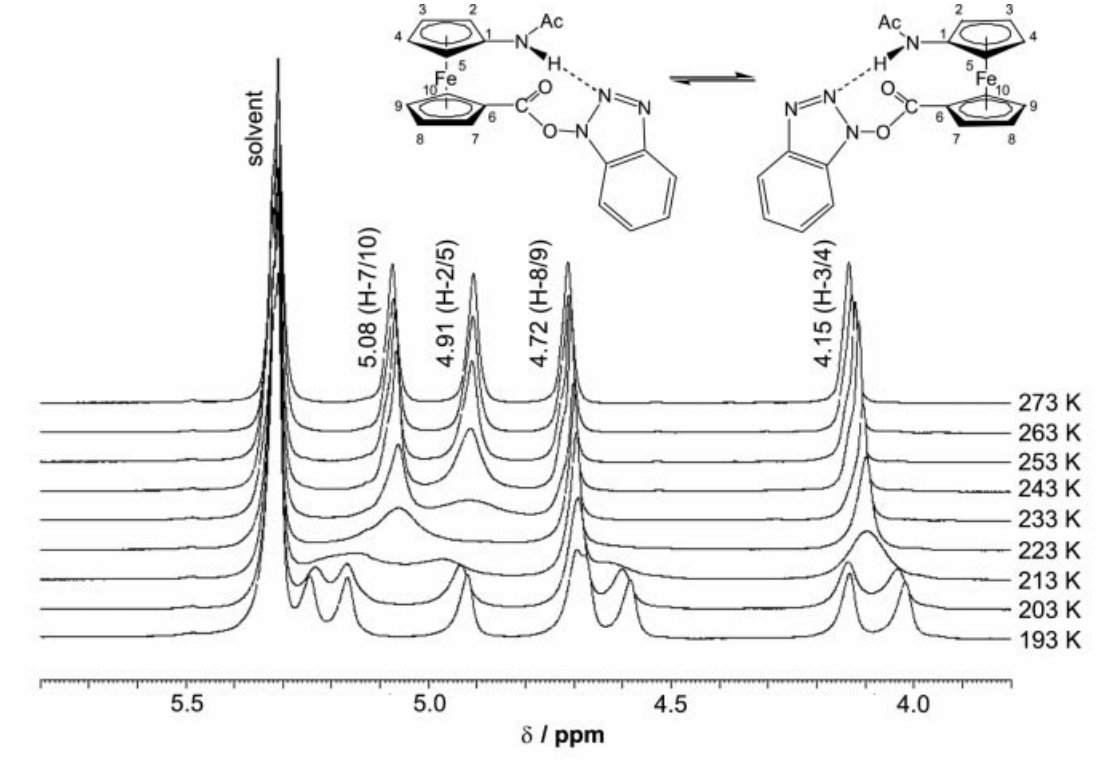

Figure 8. Partial VT-^{1}H NMR spectra of **11** (CD_2Cl_2, 500 MHz) and proposed interconversion of the enantiomeric hydrogen-bonded structures of **11**

with a charge-transfer component); the absorption band for the benzotriazole group is observed at 370 nm (Table 4). In the cyclic voltammogram the oxidation potential of the ferrocene moiety is 670 mV (Table 4).

The urea derivative **12** crystallises in the monoclinic space group $P2_1/c$ (Table 1). An intramolecular hydrogen bond from the amide proton (N1H1) to the carbonyl oxygen atom O2 is observed (N1···O2 distance: 3.02 Å, Figure 9). This intramolecular hydrogen bond in the crystal structure of **12** proves that such strongly bent connections are indeed possible (cf. proposed solution structures of **11** and **13** and the crystal structure of **11**). The molecules of **12** are connected through two different intermolecular hydrogen-bonding motifs (Figure 10): a centrosymmetric dimeric aggregate through double hydrogen bonds N1H1···O2 (N1···O2 2.96 Å), resulting in bifurcated hydrogen bonds at O2 and H1 and a connection of molecules along the *b*-axis through the NH group of urea (N3H6) and the carbonyl oxygen atom of the *N*-acetyl group (O1) with a donor acceptor distance N3···O1 of 2.95 Å.

The characteristic IR absorption bands in the solid state arise from the hydrogen-bonded NH groups (3319 cm^{-1}), CH_2 and CH groups of the cyclohexyl rings (2934, 2886 cm^{-1}), CO groups (1699, 1672, 1625 cm^{-1}) and CN groups (1569, 1543 cm^{-1}); this is consistent with the observed hydrogen bonding in the crystal structure (Table 5). In solution two absorption bands are observed for the NH stretching vibrations at 3426 and 3291 cm^{-1}. The former is assigned to the non-hydrogen-bonded NH group of the urea moiety and the latter to the hydrogen-bonded NH group of the *N*-acetyl group. Three signals assigned to the carbonyl vibrations appear at 1697, 1677 and 1619 cm^{-1}. The low-energy vibration is assigned the hydrogen-bonded carbonyl group C13−O2. Thus, the IR absorption data suggest a solution structure with an intramolecular hydrogen bond N1−H1···O2 similar to that found in the crystal (Figure 9). The IR spectroscopic data are also in agreement with the DFT-calculated frequencies of the hydrogen-bonded structure (see Supporting Information). NMR experiments confirm this proposed structure as two signals for the amide protons are observed at $\delta = 5.88$ (H^6, NOE correlation to cyclohexyl protons) and $\delta = 7.78$ (H^1), with temperature dependences of $\Delta\delta_{NH} = -13$ and -5.7 ppb K^{-1}, respectively. The large $\Delta\delta_{NH}$ observed for the urea proton H^6 is probably due to the start of intermolecular association at lower temperatures. A static structure as found for **11** was not observed for **12** in the NMR experiments at lower temperatures implying that the activation barrier for the analogous interconversion of hydrogen-bonded structures of **12** is smaller than 40 kJ mol^{-1}.

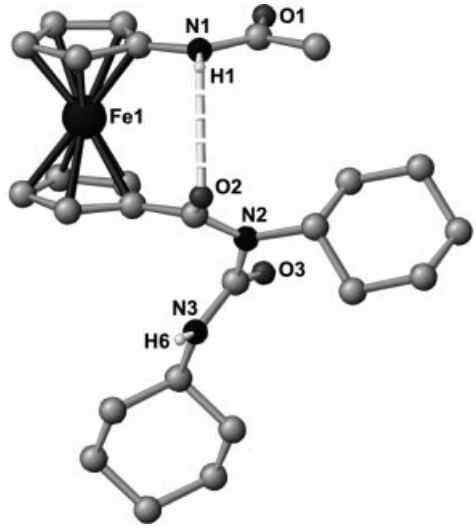

Figure 9. Molecular structure of **12** in the crystal

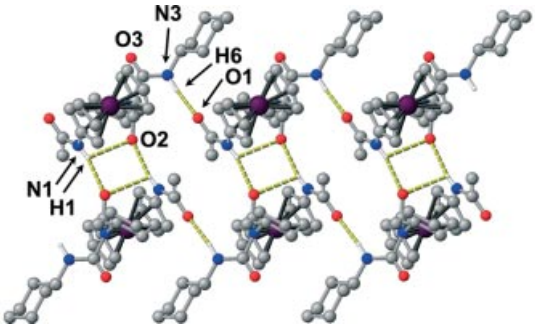

Figure 10. Hydrogen bonding of **12** in the crystal

C) Amide Formation, Crystal and Solution Structure of 13

In the activated ester **11** the C−O ester bond to the benzotriazole is very long (1.423 Å), therefore allowing a facile reaction with amines. Thus, **11** cleanly reacts with aminoferrocene **5** to give the biferrocene **13** (Scheme 6).

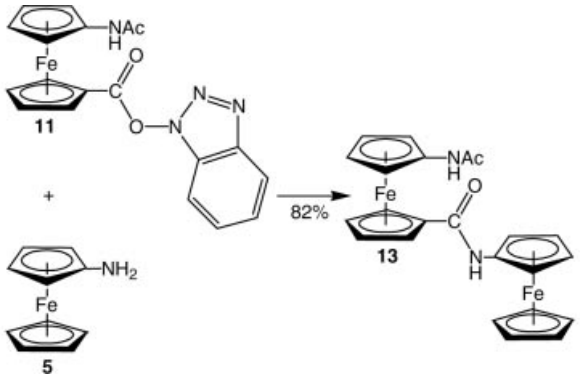

Scheme 6

The diamide **13** crystallises in the polar orthorhombic space group $P2_12_12_1$ as a twinned racemic crystal (Figure 11). The individual molecules are connected through intermolecular hydrogen bonds between the NH-acetyl group and the amide carbonyl oxygen atom (N1···O2 distance: 3.04 Å) and between the NH-amide group and the carbonyl oxygen atom of the acetyl group (N2···O1 distance: 3.03 Å) resulting in a sheet structure (Figure 12).

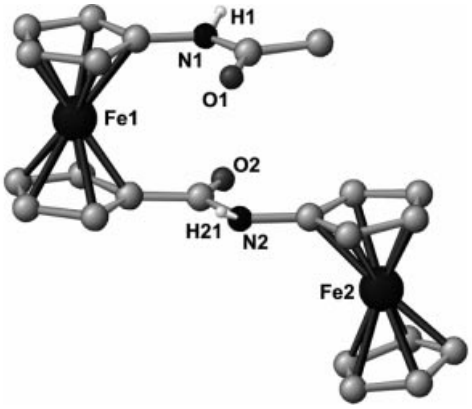

Figure 11. Molecular structure of **13** in the crystal

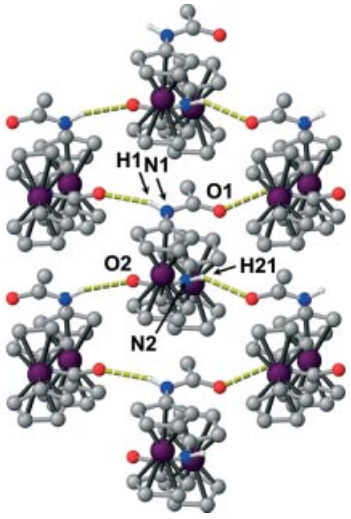

Figure 12. Hydrogen bonding of **13** in the crystal

In the solid-state IR absorption spectrum of **13** the characteristic absorption bands confirm a hydrogen-bonded structure involving all NH protons and all carbonyl groups

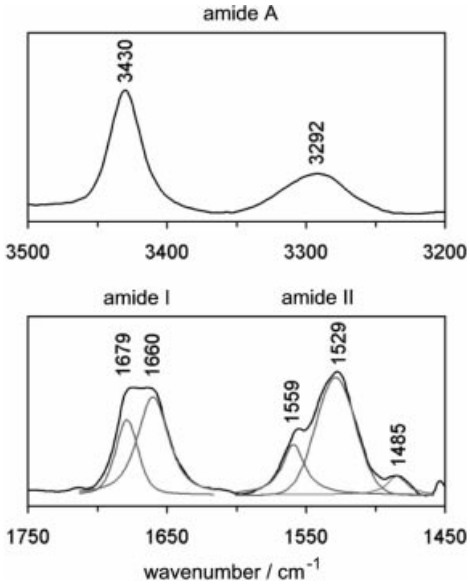

Figure 13. IR spectrum of **13** in CH_2Cl_2

(Table 5). In solution, however, one signal set for a hydrogen-bonded NHCO group (3292, 1660, 1559 cm^{-1}) and one set for a non-hydrogen-bonded NHCO group (3430, 1679, 1529 cm^{-1}) is observed (Table 5, Figure 13). These findings can be accounted for by one of the intramolecularly hydrogen-bonded structures **13a/13b**, as shown in Figure 14, or by a mixture of both structures which are indistinguishable by IR spectroscopy.

In the ^1H NMR spectrum of **13** in CD_2Cl_2 two NH resonances are observed at $\delta = 7.13$ and 8.33 with temperature dependences of $\Delta\delta_{NH} = -6.6$ and -11 ppb K^{-1}, respectively (Table 2). The former signal is assigned to the proton of the NH-acetyl group (NOESY correlation peak between CH_3 and NH) and the latter to the NH proton of the amide bond. The chemical shifts and their temperature dependences suggest that *both* protons are involved in *dynamic* hydrogen bonding. This can be rationalised by a flipping

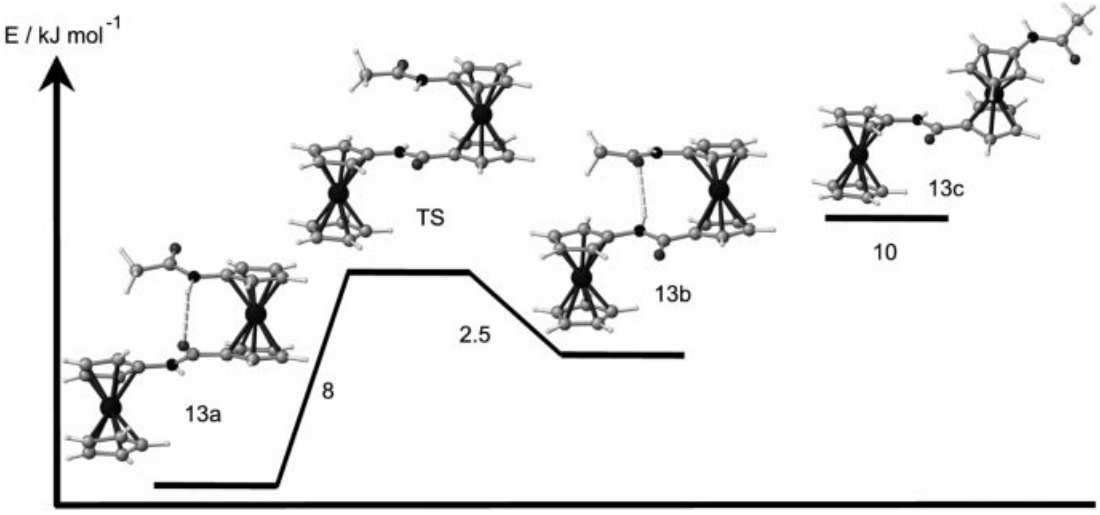

Figure 14. Interconversion of the two hydrogen-bonded structures of **13** (**13a/b**) and the extended form **13c** (DFT: B3LYP, LanL2DZ)

process that occurs between the two hydrogen-bonded structures **13a** and **13b**, as shown in Figure 14. This equilibrium is fast on the NMR time scale, averaging the NMR signals for free and hydrogen-bonded amide protons. DFT calculations on these two conformers confirm that both are minima on the potential energy surface with **13b** slightly higher in energy than **13a**. The activation barrier for the flipping process **13a** → **13b** is calculated to be only 8 kJ mol^{-1}, supporting the interpretation of a fast equilibrium (Figure 14, see Supporting Information). High-temperature NMR and IR studies show that the folded structures are stable up to 55 °C in chloroform. DFT calculations confirm the stability of **13a/13b** towards unfolding into the extended structure **13c** (Figure 14, $\Delta E_{\mathbf{13a/13c}}$ = 10 kJ mol^{-1}). From these energies, equilibrium compositions of 100:11:2 (**13a**:**13b**:**13c**) at 20 °C and 100:13:3 (**13a**:**13b**:**13c**) at 55 °C can be estimated which explain the experimental findings.

In addition to the folding characteristics imposed by the amide groups, the biferrocene compound **13** shows metal specific properties: (i) **13** absorbs at 451 nm with a small bathochromic shift relative to e.g. **12** (Table 4) and (ii) **13** can be oxidised in two reversible steps at 285 and 590 mV (Table 4). These values are different from the oxidation potentials of comparable mononuclear complexes e.g. **6** and **12** (Table 4). The constant for the comproportionation equilibrium K_C can be estimated to be 1.4×10^5, showing that $\mathbf{13^+}$ is stable towards disproportionation into **13** and $\mathbf{13^{2+}}$.

Conclusion

The optimised synthesis of the non-natural amino acid **9** reported here offers the possibility to incorporate ferrocenes in the main chain of peptides. Standard reactions of peptide synthesis (*N*-protection with Fmoc and acid activation with HOBt/DCC) have been applied to this ferrocene amino acid. The crystal structures of NHC(=O)R-substituted ferrocenes **6**−**13** have been determined by X-ray crystallography in order to elucidate hydrogen-bonding motifs. In most cases hydrogen bonding is found to be intermolecular, except in the case of the active ester **11** (only intramolecular) and the urea derivative **12** (both types). The solution structures have been investigated by a combination of IR and NMR spectroscopy, together with DFT calculations. In solution **6** and **7** are monomeric and non-hydrogen-bonded, **8** and **10** with C(=O)OH groups at the 1′ position form dimers via O−H···O and N−H···O hydrogen bonds, the active ester **11** forms an intramolecular hydrogen bond to the benzotriazole substituent, and **12** and **13** with C(=O)NRR′ groups at the 1′ position form intramolecular N−H···O hydrogen bonds. The structure of the diamide **13** in solution and in the crystal is reminiscent of the typical structures of peptides built from α-amino acids, i.e. α-helix and β-sheet structures, respectively.

This chemistry is currently extended to build ferrocene containing peptides in order to study their folding, electron-transfer and anion-sensing properties.[44]

Experimental Section

Unless noted otherwise, all manipulations were carried out under argon by means of standard Schlenk techniques. All solvents were dried by standard methods and distilled under argon prior to use. Iodoferrocene **3** was prepared by a literature method.[26] All other reagents were used as received from commercial sources. NMR spectra were recorded on Bruker Avance DPX 200 at 200.15 MHz (^{1}H), 50.323 MHz (^{13}C) at 303 K; chemical shifts (δ) in ppm with respect to residual solvent peaks as internal standards: CD_2Cl_2 (^{1}H: δ = 5.32; ^{13}C: δ = 53.5 ppm), $CDCl_3$ (^{1}H: δ = 7.24; ^{13}C: δ = 77.0 ppm), [D]$_6$DMSO (^{1}H: δ = 2.49; ^{13}C: δ = 39.7 ppm), [D]$_8$THF (^{1}H: δ = 1.73, 3.58; ^{13}C: δ = 25.5, 67.7), D_2O (^{1}H: δ = 4.65 ppm). Proton NMR spectra were measured at a concentration of 10 mM. Assignments are based on 2D NMR spectra and by comparison with spectra of similar compounds. IR absorption spectra were recorded on a BioRad Excalibur FTS 3000 spectrometer using CaF_2 cells (concentration < 10 mM) or CsI discs. UV/Vis/NIR spectra were recorded on a Perkin−Elmer Lambda 19, 0.2 cm cells (Hellma, suprasil). Cyclic voltammetry was performed using a glassy carbon electrode, a platinum electrode and a SCE electrode, 10^{-3} M in 0.1 M nBu$_4$NPF$_6$/CH_3CN, potentials are given relative to that of SCE. Mass spectra were recorded on a Finnigan MAT 8400 spectrometer, 4-nitrobenzyl alcohol (FAB). Elemental analyses were performed by the microanalytical laboratory of the Organic Chemistry Department, University of Heidelberg. Melting points were determined with a Gallenkamp capillary melting point apparatus MFB 595 010 and are uncorrected.

Computational Method: Density functional calculations were carried out with the Gaussian98/DFT[45] series of programs. The B3LYP formulation of density functional theory was used employing the LanL2DZ basis set.[45] Harmonic vibrational frequencies and infrared intensities were calculated by numerical second derivatives using analytically calculated first derivatives. Frequencies are not scaled.

Crystallographic Structure Determinations: The measurements were carried out on an Enraf−Nonius Kappa CCD diffractometer using graphite monochromated Mo-K_α radiation. The data were processed using the standard Nonius software.[46] All calculations were performed with the SHELXT PLUS software package. Structures were solved using direct or Patterson methods with the SHELXS-97 program and refined with the SHELXL-97 program.[47] Graphical handling of the structural data during refinement was performed using XMPA[48] and WinRay[49]. Atomic coordinates and anisotropic thermal parameters of the non-hydrogen atoms were refined by full-matrix least-squares calculations. Data relating to the structure determinations are collected in Table 6 and Table 7.

CCDC-225594−225602 contain the supplementary crystallographic data for this paper. These data can be obtained free of charge at www.ccdc.cam.ac.uk/conts/retrieving.html [or from the Cambridge Crystallographic Data Centre, 12 Union Road, Cambridge CB2 1EZ, UK; Fax: (internat.) +44-1223-336-033; E-mail: deposit@ccdc.cam.ac.uk].

Copper Phthalimide: (modified literature procedure)[27,28] A solution of potassium phthalimide (20 g, 107 mmol) in water (50 mL) was added to an aqueous solution of $CuSO_4 \cdot 5H_2O$ (8 g, 32 mmol) in water (50 mL). The mixture was stirred for 30 min and the resulting light blue precipitate was filtered, washed with water and ethanol and dried in vacuo. Yield: 10.8 g (93%).

2-Ferrocenylisoindole-1,3-dione (4): Copper phthalimide (20 g) and iodoferrocene (7 g, 22 mmol) were made into a powder and heated

Table 6. X-ray crystallographic data of complexes **4**, **5**, **6** and **7**

	4	**5**	**6**	**7**
Formula	$C_{18}H_{13}FeNO_2$	$C_{10}H_{11}FeN$	$C_{12}H_{10}FeNO$	$C_{19}H_{15}Cl_2FeNO_2$
Molecular mass	331.14	201.05	240.06	416.07
Crystal dimension /mm	0.15 × 0.05 × 0.05	0.15 × 0.10 × 0.05	0.10 × 0.03 × 0.03	0.15 × 0.05 × 0.05
Crystal system	monoclinic	tetragonal	monoclinic	monoclinic
Space group (no.)	$P2_1/n$ (14)	$I4_1/a$ (88)	$P2_1/n$ (14)	$P2_1/c$ (14)
a /Å	5.740(1)	23.632(3)	5.913(1)	16.027(3)
b /Å	18.406(4)	23.632(3)	7.488(2)	9.023(2)
c /Å	13.078(3)	5.931(1)	23.405(6)	11.917(2)
β /°	96.91(3)	90.0	92.44(3)	100.55(3)
Cell volume /Å^3	1371.7(5)	3312.3(9)	1035.3(4)	1694.2(6)
Molecular units per cell	4	16	4	4
μ /mm^{-1}	1.105	1.754	1.424	1.218
Density (calcd.) /g cm^{-3}	1.604	1.613	1.540	1.631
T /K	200	200	200	200
Scan range (2Θ)	3.8−54.9	3.4−55.1	5.7−55.0	5.2−55.0
Scan speed /sec frame^{-1}	20	20	40	30
Measured reflections	5748	3488	3740	6587
Unique reflections	3091	1912	2229	3862
Obs. reflections ($I \geq 2\sigma$)	1984	1202	1112	2366
Parameters refined	251	153	154	267
Max. residual electron density/e Å^{-3}	0.55/−0.53	0.31/−0.37	1.92/−0.75	0.46/−0.43
Agreement factors (F^2 refinement)	R_1 = 6.0% R_w = 15.0%	R_1 = 4.9% R_w = 11.3%	R_1 = 15.8% R_w = 40.3%	R_1 = 5.4% R_w = 12.2%

Table 7. X-ray crystallographic data of complexes **8**, **10**, **11**, **12** and **13**

	8	**10**	**11**	**12**	**13**
Formula	$C_{13}H_{13}FeNO_3{\cdot}CH_3OH$	$C_{26}H_{21}FeNO_4{\cdot}0.5CH_2Cl_2$	$C_{19}H_{16}FeN_4O_3$	$C_{26}H_{35}FeN_3O_3$	$C_{23}H_{22}Fe_2N_2O_2$
Molecular mass	319.14	509.75	404.21	493.43	470.13
Crystal dimension /mm	0.05 × 0.02 × 0.02	0.30 × 0.20 × 0.20	0.30 × 0.20 × 0.02	0.35 × 0.15 × 0.06	0.20 × 0.15 × 0.02
Crystal system	orthorhombic	monoclinic	monoclinic	monoclinic	orthorhombic
Space group (no.)	*Pbca* (61)	$P2_1/c$ (14)	$P2_1/n$ (14)	$P2_1/c$ (14)	$P2_12_12_1$ (19)
a /Å	27.396(6)	16.785(2)	9.667(2)	15.867(1)	7.489(2)
b /Å	10.228(2)	16.287(2)	16.146(3)	7.7275(6)	10.286(2)
c /Å	9.5500(19)	17.149(2)	11.253(2)	19.824(2)	24.761(5)
β /°	90.0	106.918(2)	101.85(3)	103.496(2)	90.0
Cell volume /Å^3	2676.0(9)	4485.2(8)	1719.0 (6)	2363.6(3)	1907.4(7)
Molecular units per cell	8	8	44	4	4
μ /mm^{-1}	1.139	0.827	0.906	0.665	1.544
Density (calcd.) /g cm^{-3}	1.584	1.510	1.562	1.327	1.637
T /K	200	173	200	103	200
Scan range (2Θ)	3.0−55.0	3.5−56.6	4.5−54.1	4.2−61.0	4.3−55.4
Scan speed /sec frame^{-1}	30	20	60	20	50
Measured reflections	6102	47935	6127	27762	3031
Unique reflections	3074	11134	3728	7206	3012
Obs. reflections ($I \geq 2\sigma$)	1773	8535	1920	5011	1897
Parameters refined	249	780	251	438	267
Max. residual electron density /e Å^{-3}	0.56/−0.32	0.43/−0.29	0.57/−0.30	1.58/−1.19	0.54/−0.52
Agreement factors (F^2 refinement)	R_1 = 5.3% R_w = 13.9%	R_1 = 3.4% R_w = 7.3%	R_1 = 6.5% R_w = 13.4%	R_1 = 5.2% R_w = 15.2%	6.6 17.7

in vacuo at 135−140 °C for two hours. After cooling to room temperature, the mixture was washed with petroleum ether (boiling range 40−60 °C) to remove unchanged iodoferrocene. The residue was extracted with diethyl ether (5 ×). The combined extracts were evaporated in vacuo to give an orange solid. Yield: 6 g, 18 mmol (82%). $C_{18}H_{13}NO_2Fe$ (331.15): calcd. C 65.29, H 3.96, N 4.23; found C 64.88, H 4.06, N 4.87. IR (CsI): $\tilde{\nu}$ = 3095 (w, CH), 1778 (w, CO_{sym}), 1717 (vs, CO_{asym}), 1479 (s, CN) cm^{-1}. IR (CH_2Cl_2): $\tilde{\nu}$ = 1780 (w, CO_{sym}), 1720 (vs, CO_{asym}), 1484 (s, CN) cm^{-1}. MS (FAB): *m*/*z* (%) = 331 (100) [M$^+$], 266 (64) [M$^+$ − C_5H_5]. M.p. 148−151 °C.

1-Aminoferrocene (5): Compound **4** (3.57 g, 11 mmol) was dissolved in dry ethanol (50 mL). Hydrazine monohydrate (20 mL) was added and the mixture was heated under reflux for two hours. After cooling to ambient temperature, water (80 mL) was added

and the mixture was extracted with diethyl ether (3 ×). The combined organic phases were dried over Na_2SO_4, filtered and the solvents evaporated to dryness under reduced pressure to give a yellow solid which darkens on storage. Yield: 2.2 g, 10.9 mmol (99%). $C_{10}H_{11}NFe$ (201.05): calcd. C 59.74, H 5.51, N 6.97; found C 59.64, H 5.46, N 7.07. IR (CsI): $\tilde{\nu}$ = 3400, 3336 (w, NH), 3085 (w, CH), 1621 (br., NH_{2def}), 1500 (s, CN) cm^{-1}. IR (CH_2Cl_2): $\tilde{\nu}$ = 3425, 3354 (w, NH), 1616 (br., NH_{2def}), 1497 (s, CN) cm^{-1}. MS (EI): *m/z* (%) = 201 (100) [M^+], 121 (26) [$M^+ - CpNH_2$], 80 (24) [$C_5H_6N^+$].M.p. 153−155 °C.

1-(Acetylamino)ferrocene (6): Compound **5** (2.2 g, 10.9 mmol) was treated with acetic anhydride (20 mL) in the presence of sodium acetate (0.1 g, 1.2 mmol) for 18 hours. After removal of the solvent, the crude pale brown product was purified by recrystallisation from diethyl ether/petroleum ether (40:60) to give a golden powder. Yield: 2.5 g, 10.3 mmol (95%). $C_{12}H_{13}NOFe$ (243.09): calcd. C 59.29, H 5.39, N 5.76; found C 58.80, H 5.41, N 5.81. IR (CsI): $\tilde{\nu}$ = 3262, 3216 (m, NH), 3094, 2854 (w, CH), 1655 (s, CO), 1580 (s, CN) cm^{-1}. IR (CH_2Cl_2): $\tilde{\nu}$ = 3435 (m, NH), 1685 (s, CO), 1532 (s, CN) cm^{-1}. MS (FAB): *m/z* (%) = 243 (100) [M^+]. M.p. 169−171 °C.

1-(Acetylamino)-1′-(2,6-dichlorobenzoyl)ferrocene (7): A solution of **6** (4 g, 16 mmol) in dichloromethane (30 mL) was treated with 2,6-dichlorobenzoyl chloride (2.56 mL, 16 mmol) and $AlCl_3$ (3.06 g, 23 mmol) at 0 °C. The resulting blue solution was stirred for 30 minutes at 0 °C and for two hours at room temperature. The mixture was cooled by carefully adding cold water (50 mL). The colour of the solution turned red immediately. The aqueous solution was extracted with dichloromethane (3 ×) and the combined organic phases were washed with water and 10% NaOH (aq.). After drying over $MgSO_4$ and filtering, the solution was evaporated under reduced pressure to obtain a red oil. Repeated washing with diethyl ether gave a red microcrystalline product. Yield: 4.9 g, 11.8 mmol (74%). $C_{19}H_{15}Cl_2NO_2Fe$ (416.09): calcd. C 54.85, H 3.63, N 3.37; found C 54.78, H 3.81, N 3.35. IR (CsI): $\tilde{\nu}$ = 3275, 3223 (m, NH), 3105, 2853 (w, CH), 1659 (s, CO), 1638 (sh, CO), 1574 (s, CN) cm^{-1}. IR (CH_2Cl_2): $\tilde{\nu}$ = 3431 (w, NH), 1687 (s, CO), 1655 (s, CO), 1531 (s, CN) cm^{-1}. MS (EI): *m/z* (%) = 415 (100) [M^+], 373 (22) [$M^+ - C_2H_2O$], 293 (16) [$M^+ - CpNHCOCH_3$], 178 (100) [$M^+ - CpCOAr$]. M.p. 160 °C.

1-(Acetylamino)-ferrocene-1′-carboxylic Acid (8): A solution of **7** (3.5 g, 8.4 mmol) in 1,2-dimethoxyethane (20 mL) was added to a slurry of potassium *tert*-butoxide (3.8 g, 33 mmol) and water (0.15 mL) while cooling under ice. The red solution was heated under reflux for one hour. A colour change from red to brown was observed. After cooling to ambient temperature, water (20 mL) was added and the solution was washed with diethyl ether. The organic phase was back extracted with 10% NaOH (aq.) and water. The combined aqueous phases were acidified with dilute HCl. The crude product was obtained by extraction with ethyl acetate, drying over $MgSO_4$ and evaporation to dryness. After repeated washing with diethyl ether, an orange-brown product was obtained. Yield: 1.7 g, 5.9 mmol (70%). $C_{13}H_{13}NO_3Fe$ (287.10): calcd. C 54.39, H 4.56, N 4.88; found C 54.38, H 4.55, N 4.83. IR (CsI): $\tilde{\nu}$ = 3322, 3225 (m, NH), 3300−2500 (br., OH), 1698 (sh, CO), 1666 (s, CO), 1569 (s, CN) cm^{-1}. IR (CH_2Cl_2): $\tilde{\nu}$ = 3303 (w, NH), 3235 (w, OH), 1715 (s, CO), 1691 (sh, CO), 1557 (s, CN) cm^{-1}. MS (EI): *m/z* (%) = 287 (100) [M^+], 245 (4) [$M^+ - C_2H_2O$], 178 (28) [$M^+ - CpCOOH$], 165 (4) [$M^+ - CpNHCOCH_3$], 135 (22) [$M^+ - CpCOOH - C_2H_2O$]. M.p. 146−147 °C.

1-Aminoferrocene-1′-carboxylic Acid, Hydrochloride (9·HCl): Compound **8** (0.6 g, 2 mmol) was heated under reflux in 6 N HCl (aq.) (15 mL) for 30 minutes. The mixture turned to a clear brown solution. After filtration, the solvents were evaporated to dryness and the brown residue was washed with tetrahydrofuran and diethyl ether to obtain the product as a light brown solid. Yield: 0.55 g, 1.96 mmol (98%). $C_{11}H_{11}NO_2Fe$ (245.06)·2HCl·0.5H_2O: calcd. C 40.41, H 4.32, N 4.28; found C 39.98, H 4.52, N 4.78. IR (CsI): $\tilde{\nu}$ = 3366 (vs, OH), 3177, 3135, 3030 (m, NH_3^+), 1628 (m, CO) cm^{-1}. MS (FAB): *m/z* (%) = 245 (100) [M^+], 228 (24) [$M^+ - NH_4$]. M.p. 165 °C (dec.).

1-[(Fluoren-9-yl)methyloxycarbonylamino]ferrocene-1′-carboxylic Acid (10): 1-Aminoferrocene-1′-carboxylic acid, hydrochloride **9·HCl** (1.1 g, 3.9 mmol) was dissolved in phosphate buffer (20 mL) and the pH was adjusted to 7. 9-Fluorenylmethyl chloroformate (1.03 g, 3.98 mmol) dissolved in dioxane (10 mL) was added to the solution. A bright orange solid separated from the solution immediately after the addition. After stirring overnight, the precipitate was collected by filtration and washed twice with diethyl ether. Recrystallisation from dichloromethane gave an orange powder. Yield: 1.5 g, 3.2 mmol (82%). $C_{26}H_{21}NO_4Fe$ (467.30)·0.5CH_2Cl_2: calcd. C 62.44, H 4.35, N 2.75; found C 62.25, H 4.34, N 2.87. IR (CsI): $\tilde{\nu}$ = 3263, 3153 (m, NH), 3400−2800 (br., OH), 1707 (s, CO), 1664 (s, CO), 1560 (w, CN) cm^{-1}. IR (CH_2Cl_2): $\tilde{\nu}$ = 3425, 3316 (w, NH), 3266 (w, OH), 1735 (s, CO), 1707 (s, CO), 1673 (s, CO), 1570, 1544 (m, CN) cm^{-1}. IR (THF): $\tilde{\nu}$ = 3573, 3504 (w, NH), 3269 (w, OH), 1735 (s, CO), 1717 (s, CO), 1563 (m, CN) cm^{-1}. MS (FAB): *m/z* (%) = 467 (100) [M^+]. M.p. 118 °C.

Benzotriazol-1-yl 1-(Acetylamino)ferrocene-1′-carboxylate (11): Dicyclohexylcarbodiimide (0.86 g, 4.2 mmol) and *N*-hydroxybenztriazole (0.415 g, 4.2 mmol) was added to a solution of **8** (1.1 g, 3.8 mmol) in dichloromethane (10 mL). The mixture was stirred at room temperature overnight. After filtering, the solution was washed with aqueous $NaHCO_3$, saturated NaCl (aq.) and 2% HCl (aq.). After drying over $MgSO_4$, the solvent was removed in vacuo and the crude product was purified by column chromatography on silica gel with ethyl acetate as eluent. After removal of the solvent under reduced pressure an orange red powder was obtained. Yield: 1.23 g, 3.0 mmol (80%). $C_{19}H_{16}N_4O_3Fe$ (404.21): calcd. C 56.46, H 3.99, N 13.86; found C 57.13, H 4.47, N 13.17. IR (CsI): $\tilde{\nu}$ = 3359 (m, NH), 1764 (s, CO), 1682 (s, CO), 1548 (s, CN), 1491 (m) cm^{-1}. IR (CH_2Cl_2): $\tilde{\nu}$ = 3428, 3363 (w, NH), 1787 (s, CO), 1689 (s, CO), 1536 (s, CN),1485(m) cm^{-1}. MS (FAB): *m/z* (%) = 404 (100) [M^+]. M.p. 133 °C.

1-[1′-(Acetylamino)ferrocenylcarbonyl]-1,3-dicyclohexylurea (12): Compound **8** (1.02 g, 3.5 mmol) was dissolved in tetrahydrofuran (20 mL) and 1,3-dicyclohexylcarbodiimide (0.73 g, 3.5 mmol) was added to the stirred solution. After standing overnight at room temperature, the solvent was removed in vacuo and the crude product was purified by column chromatography on silica gel with ethyl acetate as eluent. The solvent was removed under reduced pressure and an orange-brown product was obtained. Yield: 1.46 g, 3.0 mmol (85%). $C_{26}H_{35}N_3O_3Fe$·0.18CH_2Cl_2 (493.43·0.18CH_2Cl_2): calcd. C 61.80, H 7.00, N 8.26; found C 61.84, H 6.75, N 7.85. IR (CsI): $\tilde{\nu}$ = 3319 (s, NH), 2934 (vs, CH_2), 2856 (s, CH), 1699 (s, CO), 1672 (vs, CO), 1625 (s, CO), 1569 (s, CN), 1541 (m, CN) cm^{-1}. IR (CH_2Cl_2): $\tilde{\nu}$ = 3426 (m, NH), 3291 (m, NH), 2936 (s, CH_2), 2858 (m, CH), 1697 (s, CO), 1677 (s, CO), 1619 (m, CO), 1526 (s, CN), 1510 (s, CN) cm^{-1}. MS (FAB): *m/z* (%) = 493 (20) [M^+], 368 (93) [$M^+ - CyNCO$], 178 (100) [FeCpNHAc]. M.p. 158 °C.

($CH_3CONH-C_5H_4$)Fe(C_5H_4-$CONH-C_5H_4$)Fe(C_5H_5) (13): Compound **11** (1.20 g, 2.9 mmol) and aminoferrocene **5** (0.59 g, 2.9 mmol) were dissolved in tetrahydrofuran (10 mL) and stirred

for 12 h at ambient temperature. The solvent was removed in vacuo and the residue was dissolved in dichloromethane. The solution was washed with water, aqueous $NaHCO_3$, saturated NaCl and 2% HCl. The organic layer was dried over $MgSO_4$ and the solvent was removed under reduced pressure. Recrystallisation from dichloromethane gave an orange-brown product. Yield: 1.1 g, 2.4 mmol (82%). $C_{23}H_{22}N_2O_2Fe_2$ (470.13): calcd. C 58.76, H 4.72, N 5.96; found C 58.51, H 5.53, N 6.40. IR (CsI): $\tilde{\nu}$ = 3327, 3316 (m, NH), 1660 (s, CO), 1646 (s, CO), 1560 (vs, CN) cm^{-1}. IR (CH_2Cl_2): $\tilde{\nu}$ = 3430, 3292 (w, NH), 1679, (s, CO), 1660 (s, CO), 1559, 1529 (s, CN), 1485 (w) cm^{-1}. MS (FAB): *m*/*z* (%) = 470 (100) [M^+], 405 (38) [M^+ − Cp]. M.p. 196 °C.

Acknowledgments

This work was supported by the Deutsche Forschungsgemeinschaft and the Fonds der Chemischen Industrie. The permanent, generous support from Prof. Dr. G. Huttner is gratefully acknowledged. We thank Simone Leingang for preparative assistance.

[1] H.-A. Klok, *Angew. Chem. Int. Ed.* **2002**, *114*, 1579−1583; *Angew. Chem. Int. Ed.* **2002**, *41*, 1509−1513.
[2] P. Nguyen, P. Gómez-Elipe, I. Manners, *Chem. Rev.* **1999**, *99*, 1515−1548.
[3] D. T. Bong, T. D. Clark, J. R. Granja, M. R. Ghadiri, *Angew. Chem. Int. Ed.* **2001**, *113*, 1016−1041; *Angew. Chem. Int. Ed.* **2001**, *40*, 988−1011.
[4] A. Aggeli, M. Bell, N. Boden, J. N. Keen, P. F. Knowles, T. C. B. McLeish, M. Pitkeathly, S. E. Radford, *Nature* **1997**, *386*, 259−262.
[5] T. C. Holmes, S. de Lacalle, X. Su, G. Liu, A. Rich, S. Zhang, *Proc. Natl. Acad. Sci. USA* **2000**, *97*, 6728−6733.
[6] T. J. Peckham, P. Gómez-Elipe, I. Manners in *Metallocenes* (Eds.: A. Togni, R. L. Haltermann), Wiley-VCH, Weinheim, **1998**, pp. 723−771.
[7] P. D. Beer, *Acc. Chem. Res.* **1998**, *31*, 71−80.
[8] P. D. Beer, J. J. Davis, D. A. Drillsma-Milgrom, F. Szemes, *Chem. Commun.* **2002**, 1716−1717.
[9] T. Ihara, M. Nakayama, M. Murata, K. Nakano, M. Maeda, *Chem. Commun.* **1997**, 1609−1610.
[10] K. Kavallieratos, S. Hwang, R. H. Crabtree, *Inorg. Chem.* **1999**, *38*, 5184−5186.
[11] K. Severin, R. Bergs, W. Beck, *Angew. Chem. Int. Ed.* **1998**, *110*, 1722−1743, *Angew. Chem. Int. Ed.* **1998**, *37*, 1634−1654.
[12] O. Brosch, T. Weyhermüller, N. Metzler-Nolte, *Inorg. Chem.* **1999**, *38*, 5308−5313.
[13] D. R. van Staveren, T. Weyhermüller, N. Metzler-Nolte, *Dalton Trans.* **2003**, 210−220.
[14] A. Nomoto, T. Moriuchi, S. Yamazaki, A. Ogawa, T. Hirao, *Chem. Commun.* **1998**, 1963−1964.
[15] T. Moriuchi, A. Nomoto, K. Yoshida, T. Hirao, *Organometallics* **2001**, *20*, 1008−1013.
[16] T. Moriuchi, A. Nomoto, K. Yoshida, A. Ogawa, T. Hirao, *J. Am. Chem. Soc.* **2001**, *123*, 68−75.
[17] T. Muraoka, K. Kinbara, Y. Kobayashi, T. Aida, *J. Am. Chem. Soc.* **2003**, *125*, 5612−5613.
[18] E. S. Stevens, N. Sugawara, G. M. Bonora, C. Toniolo, *J. Am. Chem. Soc.* **1980**, *102*, 7048−7050.
[19] *Fmoc Solid Phase Peptide Synthesis* (Eds.: W. C. Chan, P. D. White), Oxford University Press, Oxford, **2000**.
[20] J. R. Butler, S. C. Quayle, *J. Organomet. Chem.* **1998**, *552*, 63−68.
[21] T. Okamura, K. Sakauye, N. Ueyama, A. Nakamura, *Inorg. Chem.* **1998**, *37*, 6731−6736.
[22] L. Barisić, V. Rapić, V. Kovač, *Croat. Chem. Acta* **2002**, *75*, 199−210.
[23] D. W. Hall, J. H. Richards, *J. Org. Chem.* **1963**, *28*, 1549−1554.
[24] D. C. D. Butler, C. J. Richards, *Organometallics* **2002**, *21*, 5433−5436.
[25] M. Herberhold, M. Ellinger, W. Kremnitz, *J. Organomet. Chem.* **1983**, *241*, 227−240.
[26] B. Bildstein, M. Malaun, H. Kopacka, K. Wurst, M. Mitterböck, K.-H. Onania, G. Opromolla, P. Zanello, *Organometallics* **1999**, *18*, 4325−4336.
[27] A. N. Nesmeyanov, W. A. Ssazonova, D. N. Drosa, *Chem. Ber.* **1960**, *93*, 2717−2729.
[28] N. Monserrat, A. W. Parkins, A. R. Tomkins, *J. Chem. Res. Synop.* **1995**, 336−337.
[29] M. Derenberg, P. Hodge, *Tetrahedron. Lett.* **1971**, *41*, 3825−3828.
[30] C. J. McAdam, B. H. Robinson, J. Simpson, *Organometallics* **2000**, *19*, 3644−3653.
[31] A. Shafir, M. P. Power, G. D. Whitener, J. Arnold, *Organometallics* **2000**, *19*, 3978−3982.
[32] K. Kam-Wing Lo, J. Shing-Yip Lau, D. Chun-Ming Ng, N. Zhu, *J. Chem. Soc., Dalton Trans.* **2002**, 1753−1756.
[33] G. Pavlović, L. Barisić, V. Rapić, I. Leban, *Acta Crystallogr., Sect. E* **2002**, *58*, m13−m15.
[34] S. Lu, V. V. Strelets, M. F. Ryan, W. J. Pietro, A. B. P. Lever, *Inorg. Chem.* **1996**, *35*, 1013−1023.
[35] Semiempirical ZINDO calculations confirm this assignment: see for example: D. R. Kanis, M. A. Ratner, T. J. Marks, *J. Am. Chem. Soc.* **1990**, *112*, 8203−8204.
[36] W. Koch, M. C. Holthausen, *A Chemist's Guide to Density Functional Theory*, Wiley-VCH, Weinheim, **2001**.
[37] G. Pavlović, L. Barisić, V. Rapić, V. Kovač, *Acta Crystallogr., Sect. C* **2003**, *59*, m55−m57.
[38] *cis*/*trans*-Conformers of urethane derivatives have been observed in the crystal: H. Oku, K. Yamada, R. Katakai, *Acta Crystallogr., Sect. E* **2003**, *59*, o1130−o1132.
[39] *cis*/*trans*-Conformers of Fmoc protected amino acids have been observed in solution: G. Valle, G. M. Bonora, C. Toniolo, *Can. J. Chem.* **1984**, *62*, 2661−2666.
[40] H.-B. Kraatz, J. Lusztyk, G. D. Enright, *Inorg. Chem.* **1997**, *36*, 2400−2405.
[41] A. F. Neto, J. Miller, V. Faria de Andrade, S. Yumi Fujimoto, M. M. de Freitas Alfonso, F. C. Archanjo, V. A. Darin, M. L. Andrade de Silva, Á. D. L. Borges, G. Del Ponte, *Z. Anorg. Allg. Chem.* **2002**, *628*, 209−216.
[42] E. M. Acton, R. M. Silverstein, *J. Org. Chem.* **1959**, *24*, 1487−1490.
[43] H. H. Lau, H. Hart, *J. Org. Chem.* **1959**, *24*, 280−281.
[44] P. D. Beer, P. A. Gale, *Angew. Chem. Int. Ed.* **2001**, *113*, 502−532; *Angew. Chem. Int. Ed.* **2001**, *40*, 486−516.
[45] M. J. Frisch, G. W. Trucks, H. B. Schlegel, G. E. Scuseria, M. A. Robb, J. R. Cheeseman, V. G. Zakrzewski, J. A. Montgomery Jr., R. E. Stratmann, J. C. Burant, S. Dapprich, J. M. Millam, A. D. Daniels, K. N. Kudin, M. C. Strain, O. Farkas, J. Tomasi, V. Barone, M. Cossi, R. Cammi, B. Mennucci, C. Pomelli, C. Adamo, S. Clifford, J. Ochterski, G. A. Petersson, P. Y. Ayala, Q. Cui, K. Morokuma, D. K. Malick, A. D. Rabuck, K. Raghavachari, J. B. Foresman, J. Cioslowski, J. V. Ortiz, B. B. Stefanov, G. Liu, A. Liashenko, P. Piskorz, I. Komaromi, R. Gomperts, R. L. Martin, D. J. Fox, T. Keith, M. A. Al-Laham, C. Y. Peng, A. Nanayakkara, C. Gonzalez, M. Challacombe, P. M. W. Gill, B. Johnson, W. Chen, M. W. Wong, J. L. Andres, C. Gonzalez, M. Head-Gordon, E. S. Replogle, J. A. Pople, Gaussian 98, revision A.6, Gaussian, Inc., Pittsburgh PA, **1998**, http://www.gaussian.com.
[46] R. Hooft, Collect, Data Collection Software, Nonius, The Netherlands, **1998**, http://www. nonius. com.
[47] G. M. Sheldrick, *SHELXS-97, Program for Crystal Structure Solution*, University of Göttingen, Germany, **1997**, http://www.shelx.uni-ac.gwdg.de/shelx/index.html; G. M. Sheldrick, *SHELXL-97, Program for Crystal Structure Refinement*, University of Göttingen, Germany, **1997**, http://www.shelx.uni-

ac.gwdg.de/shelx/index.html; *International Tables for X-ray Crystallography*, Kynoch Press, Birmingham, U. K., **1974**, vol. 4.
[48] L. Zsolnai, G. Huttner, *XPMA*, University of Heidelberg, Germany, **1998**, http://www.rzuser.uni-heidelberg.de/~il1/laszlo/xpm.html.
[49] R. Soltek, G. Huttner, *WinRay*, University of Heidelberg, Germany, **1999**, http://www.uni-heidelberg.de/institute/fak12/AC/huttner/frame/frame_soft.html

Received December 4, 2003
Early View Article
Published Online May 13, 2004

